LMSC-A324768
10 June 1963

PROGRAM 461 TELEMETRY ALIASING ERROR ANALYSIS

APPROVED:

E. SCHAEFER, MANAGER
PROGRAM 461 C&C SYSTEM

APPROVED:

J. C. SOLVASON, MANAGER
PROGRAM 461

FOREWORD

This report is published by Lockheed Missiles and Space Company, Space Systems Division, under Contract AF 04(647)-787. It presents the results of a computer simulation of Program 461 payload telemetry system in a form which enables the designer to determine data sampling rate and number of channels for a given aliasing error allocation.

CONTENTS

CONTENTS (Continued)

ILLUSTRATIONS

INTRODUCTION AND SUMMARY

Aliasing error occurs when interpolation is applied to data samples whose period between samples is too great to recover the higher frequency components in the data spectrum. Since the data spectrum generally contains high frequency components which are not of interest, the signal is low-pass filtered to attenuate the undesirable portion of the spectrum. It is this portion, although attenuated, that "folds" about the Nyquist frequency thereby causing aliasing error.

Aliasing error may be reduced by faster sampling and/or better filtering. Since it is mandatory that a high degree of accuracy be attained with a minimum sampling rate, an optimization analysis is clearly necessary. To accomplish this, the telemetry system is described mathematically by the transfer functions of its significant blocks. Previously, a cursory analysis was performed by using graphical integration (Ref 1). This effort led to a more mathematically refined approach with the calculations being performed by an IBM 7094 computer.

Mathematical functions are derived for the Program 461 payload telemetry system, and utilized to compute rms aliasing error versus data sampling rate. Three different interpolation filter types are compared; a physically realizable Butterworth, an ideal rectangular shape with infinite slope, and an optimum filter whose characteristics are a function of the data spectrum. Both the high resolution and low resolution channels are analyzed. The computation was performed on an IBM 7094 computer, with a program written so that system parameters could be easily varied.

For the two blur-circle time functions assumed, Gaussian and cosine-squared, curves of rms aliasing error versus sampling frequency are developed. Finally, for a given aliasing error, interpolation filter, and input spectrum, the allowable number of low and high resolution channels are shown.

SECTION 1
DESCRIPTION OF TELEMETRY SYSTEM

1.1 BLOCK DIAGRAM

Figure 1-1 shows the significant blocks of the system, the voltage transfer functions, and the sampling functions.

1.2 OPTICS

When a point source is viewed by the optical system, the energy distribution of the image forms a blur-circle whose mathematical expression is a function of the optical parameters. As the blur-circle moves across the detector aperture, the energy versus time curve assumes a shape somewhere between a Gaussian and a cosine-squared pulse. Figure 1-2 shows the frequency spectrum for both cases.

1.2.1 Case I - Gaussian Pulse

$$h_o\left(t\right) = \frac{A}{t_1\sqrt{2\pi}} \epsilon^{-1/2\left(\frac{t}{t_1}\right)^2} \quad , -\infty < t < +\infty$$

It was assumed (Ref 1) that since 95 percent of the image is contained within the detector aperture and the scan time across the aperture is $\frac{1}{720}$ seconds, $t_1 = 1/4\left(\frac{1}{720}\right)$. This is due to the fact that 95 percent of the energy in a Gaussian pulse is contained within $-2\sigma \leq t \leq +2\sigma$. The frequency function or spectrum of the Gaussian pulse is also Gaussian and equal to:

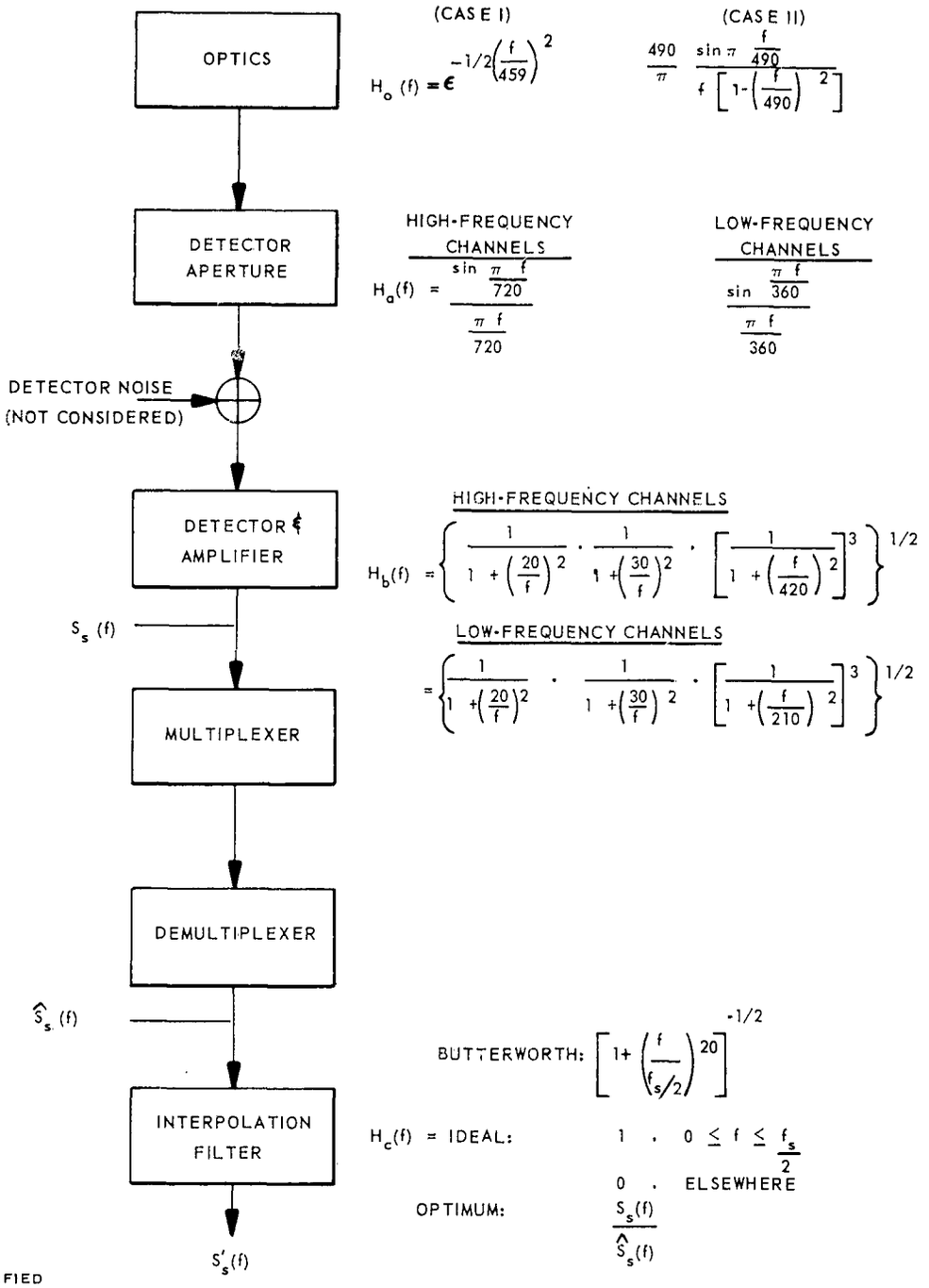

Figure 1-1 System Block Diagram

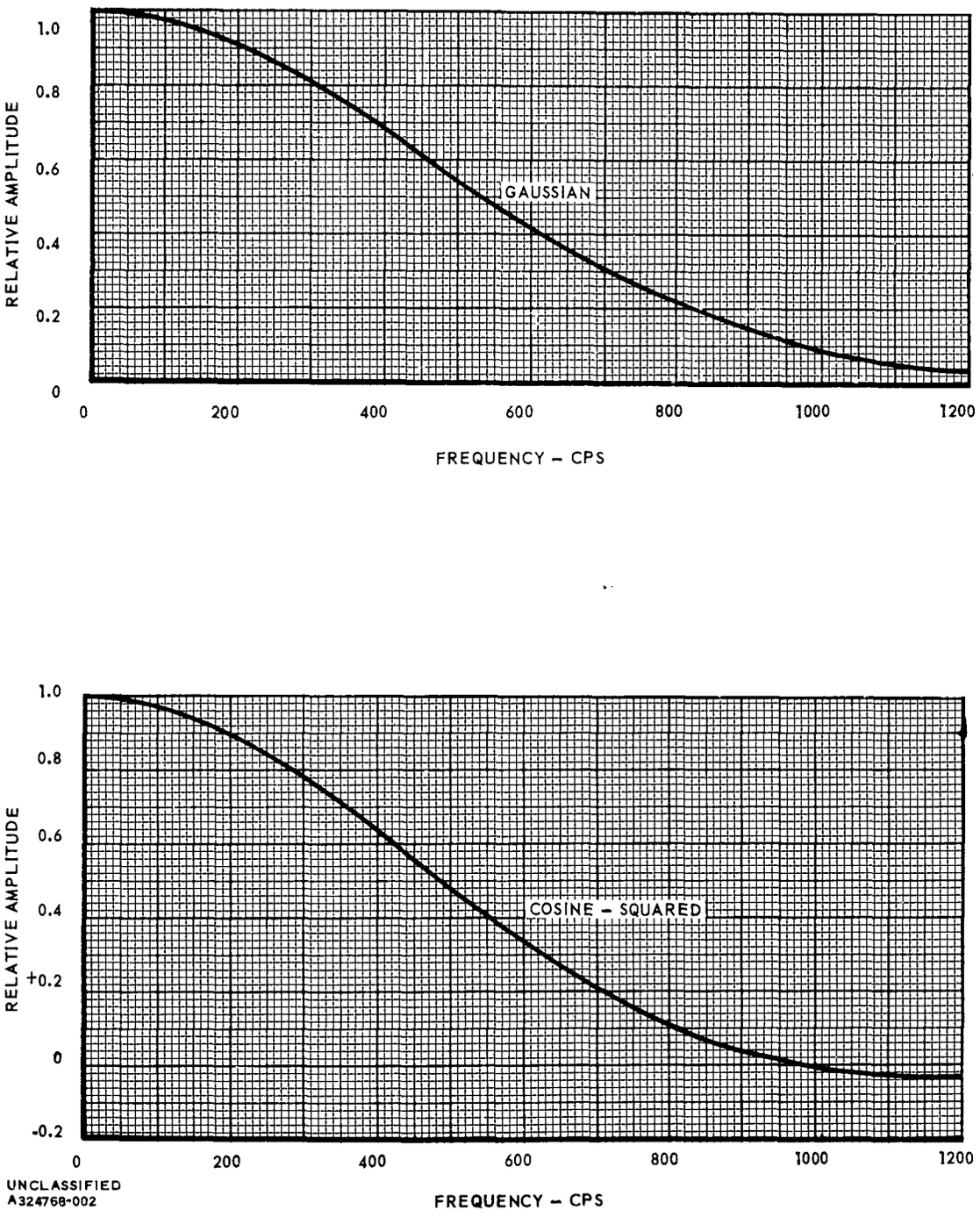

Figure 1-2 Frequency Spectrum of Assumed Blur-Circle Time Functions

$$H_o\left(f\right) = A\epsilon^{-1/2\left(2\pi t_1 f\right)^2}$$

$$= A\epsilon^{-1/2\left(\frac{f}{459}\right)^2}$$

1.2.2 Case II - Cosine-Squared-Pulse

$$h_o\left(t\right) = \frac{2A}{t_o}\cos^2\pi\frac{t}{t_o}, \quad -\frac{t_o}{2} \leq t \leq +\frac{t_o}{2}$$

$$= 0, \text{ elsewhere}$$

Again for this case, 95 percent of the image is assumed to be contained within the detector aperture; consequently $t_o = \frac{1}{490}$ (Appendix A). The normalized frequency function is:

$$H_o\left(f\right) = \frac{490\,A}{\pi}\,\frac{\sin\frac{\pi f}{490}}{f\left[1 - \left(\frac{f}{490}\right)^2\right]}$$

1.3 DETECTOR APERTURE

Since the detector shape is rectangular, a sweep across the aperture would result in a rectangular time function:

$$h_A\left(t\right) = \frac{A}{t_o}, \quad -\frac{t_o}{2} \leq t \leq +\frac{t_o}{2}$$

$$= 0, \text{ elsewhere}$$

Since the sweep across the aperture is $\frac{1}{720}$ seconds for the high resolution channels and $\frac{1}{360}$ seconds for the low resolution channels, $t_o = \frac{1}{720}$ and $\frac{1}{360}$ respectively. The frequency function is:

$$H_A\left(f\right) = A \frac{\sin \frac{\pi f}{t_o}}{\frac{\pi f}{t_o}}$$

1.4 DETECTOR AND AMPLIFIER

The frequency function, in the case of the high resolution channels, for the detector-amplifier combination was derived from the idealistic shape as shown in Figure 1-3. Two situations were postulated; one in which the high frequency roll-off of the existing amplifier is 18 db/octave, and one in which the roll-off is increased to 24 db/octave. Since the amplifier is composed of R-C coupling networks, the equation for the gain across the band is easily formed. For N = 3 and N = 4, the high frequency -3 db point is 214 cps and 183 cps respectively. However, the curve is still asymptotic to the slope as illustrated in Figure 1-2.

$$H_o\left(f\right) = \left\{ \left[\frac{1}{1+\left(\frac{20}{f}\right)^2}\right]\left[\frac{1}{1+\left(\frac{30}{f}\right)^2}\right]\left[\frac{1}{1+\left(\frac{f}{420}\right)^2}\right]^N \right\}^{1/2}$$

Where N = 3 for 18 db/octave roll-off, and N = 4 for 24 db/octave roll-off.

In the case of the low resolution channels, the high frequency pole is reduced from 420 to 210 cps.

1.5 MULTIPLEXER

Ideally, the multiplexer samples the data repetitively with zero dwell time thereby producing a series of delta functions of magnitude equal to the magnitude of the data

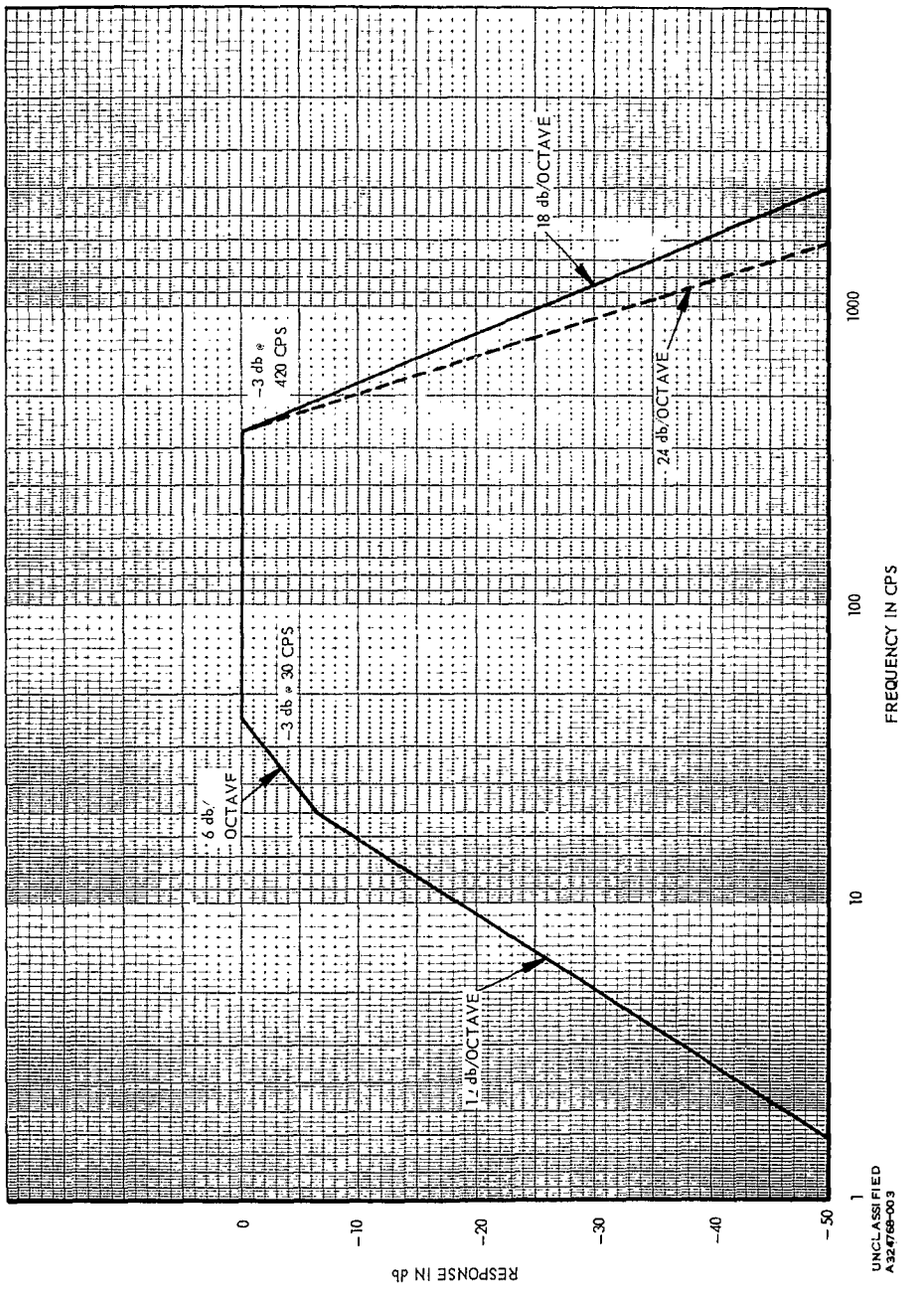

Figure 1-3 High Resolution Channels Amplifier-Detector Frequency Response, Idealized

at the sampling time. Consequently, if only the peak value of the data is desired, the error would be zero if the effect of finite dwell time is not considered. However, since the spectrum of the data is to be reproduced, interpolation between data samples must be applied and error is inherent. The effect of finite dwell time is to introduce frequency distortion in the recovered data. The method of determining the magnitude of the error is explained in Reference 1. The error is 0.004 percent, with typical system parameters (Appendix B). The sampling function ideally is:

$$\hat{S}_s\left(f\right) = \sum_{n=0}^{\infty} S_s\left(f - n f_s\right)$$

where

$\hat{S}_s\left(f\right)$ = Sampled data power system

$S_s\left(f\right)$ = data power spectrum

f_s = sampling frequency

1.6 DEMULTIPLEXER

The demultiplexer merely decommutates the composite signal and has no effect upon the aliasing error.

1.7 INTERPOLATION FILTER

The three interpolation filter characteristics, which were considered, are listed below.

1.7.1 Ideal Filter

The ideal, rectangular shaped filter, with infinite slope at half the sampling frequency, is easy to simulate with the computer. Its function is:

$$H_o\left(f\right) = 1, \quad 0 \leq f \leq \frac{f_s}{2}$$

$$= 0, \text{ elsewhere}$$

1.7.2 Butterworth Filter

A 10-pole 60 db/octave Butterworth filter, which is physically realizable, is given by the function:

$$H_o\left(f\right) = \left[1 + \left(\frac{f}{f_s/2}\right)^{20}\right]^{-1/2}$$

1.7.3 Optimum Filter

The optimum filter, as derived by Spilker (Ref 2), is of the form:

$$H_c\left(f\right) = \frac{S_s\left(f\right)}{\hat{S}_s\left(f\right)}$$

Realization of this filter depends upon a-priori knowledge of the data spectrum; consequently, we may only approach optimum in actual practice.

SECTION 2
METHOD OF ANALYSIS

The method of analysis following that of J. J. Downing's work (Ref 3), along with the system transfer functions described previously, gives an exact calculation of the aliasing error.

2.1 MEAN-SQUARED ERROR

The sampled data spectrum may be written as:

$$\hat{S}_s\left(f\right) = S_s\left(f\right) + S_n\left(f\right)$$

where

$$S_n\left(f\right) = \sum_{n=1}^{\infty} S_s\left(f - n f_s\right)$$

For a general interpolation filter with voltage transfer function $H_c\left(f\right)$, the mean-squared error is:

$$\overline{\epsilon^2} = \int_{-\infty}^{+\infty} \left\{ S\left(f\right) - 2 S_s\left(f\right) H_c\left(f\right) + \left|H_c\left(f\right)\right|^2 \hat{S}_s\left(f\right) \right\} df$$

For the optimum interpolation filter, the mean-squared error is:

$$\overline{\epsilon_o^2} = \int_{-\infty}^{+\infty} \frac{S_s\left(f\right) S_n\left(f\right)}{\hat{S}_s\left(f\right)} df$$

where the optimum filter transfer function is given by:

$$H_c(f) = \frac{S_s(f)}{\hat{S}_s(f)}$$

2.2 NORMALIZED ERROR

The error was normalized with respect to the data power spectrum

$$E_{rms} = \left[\frac{\overline{\epsilon^2}}{\int_{-\infty}^{+\infty} S_s(f)\,df} \right]^{1/2}$$

and expressed as percent rms aliasing error in the subsequent curves.

SECTION 3
RESULTS OF COMPUTER ANALYSIS

To facilitate IBM 7094 computer analysis the sampled data spectrum was summed to 2.5 f_s and the mean-squared error was integrated from 0 to 2.5 f_s and multiplied by 2 as allowed by symmetry. Since the roll-off of the assumed interpolation filter is quite sharp (infinite in the case of the ideal filter), negligible improvement is gained by summing and integrating further than 2.5 f_s. The operations were performed in 50 cycle increments in order to give realistic results while keeping machine time reasonable.

3.1 ALIASING ERROR VS SAMPLING FREQUENCY

3.1.1 High Resolution Channels

Figures 3-1 and 3-2 show the rms aliasing error for three interpolation filters when the input time function is Gaussian. Figures 3-3 and 3-4 show the rms aliasing error for the three interpolation filters when the input time function is cosine-squared.

The rms aliasing error is slightly less for the cosine-squared function, due to less high frequency energy in the data spectrum, than for the Gaussian function. This comparison may be made by referring to Figure 1-2, and noting the difference between the two curves.

3.1.2 Low Resolution Channels

Figures 3-5 and 3-6 show the results of the analysis when the aperture and amplifier functions are modified for the case of low resolution channels (Gaussian input pulse). Figures 3-7 and 3-8 show the rms aliasing error for the low resolution channels when the input time function is cosine-squared.

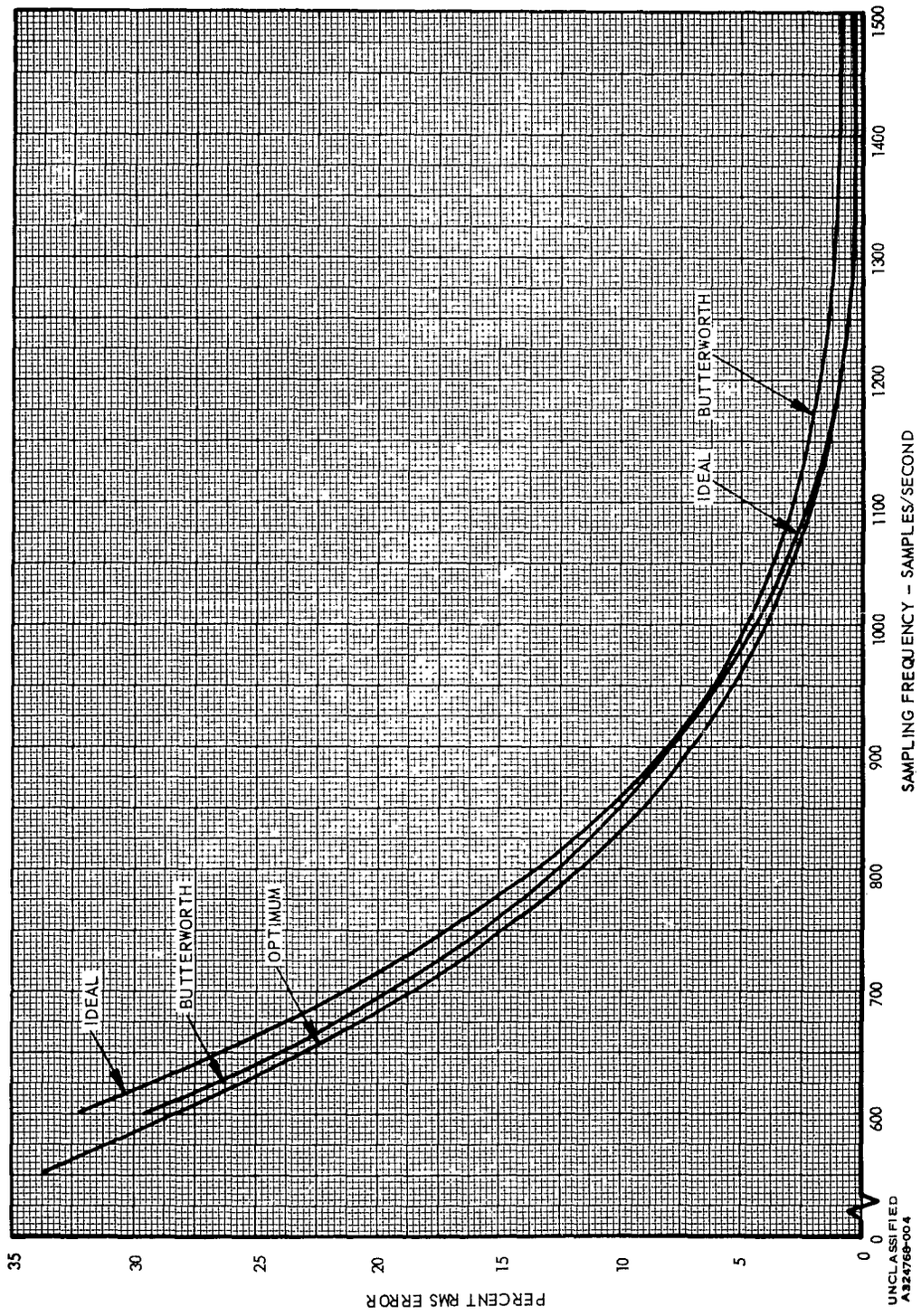

Figure 3-1 Aliasing Error vs Sampling Frequency – High Resolution Channels (Gaussian Input Function)

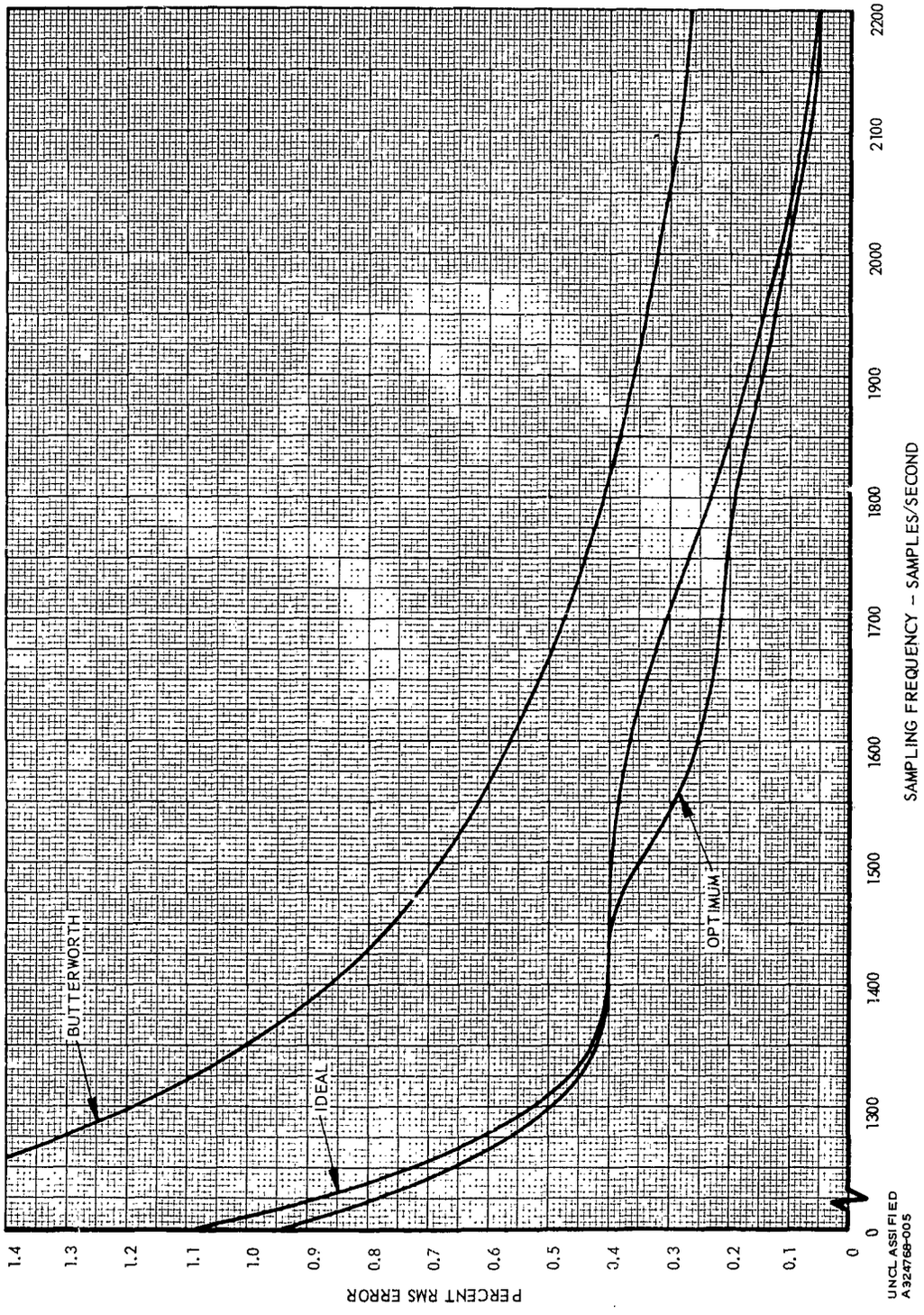

Figure 3-2 Aliasing Error vs Sampling Frequency - High Resolution Channels: Expanded (Gaussian Input Function)

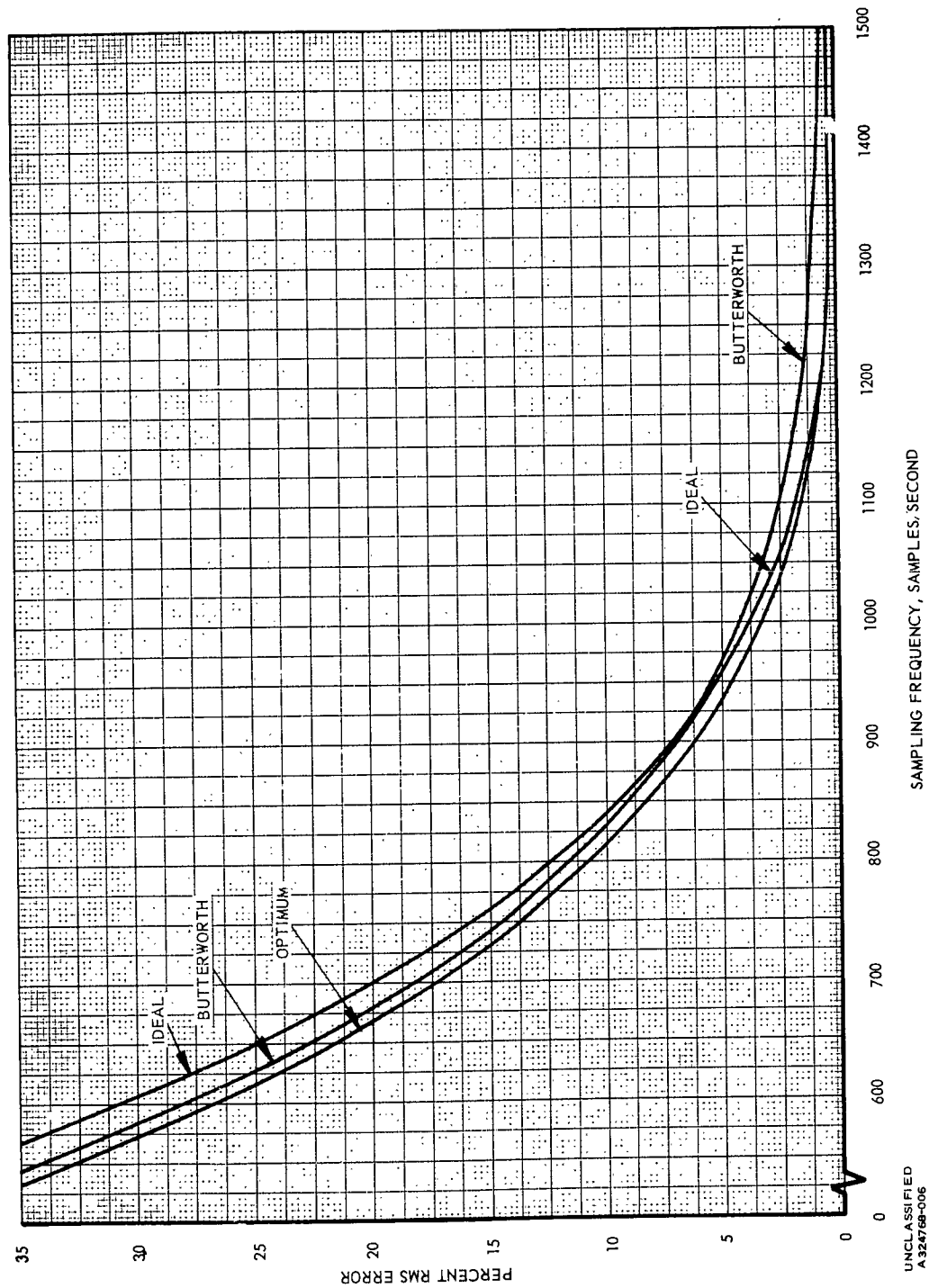

Figure 3-3 Aliasing Error vs Sampling Frequency - High Resolution Channels (Cosine-Squared Input Function)

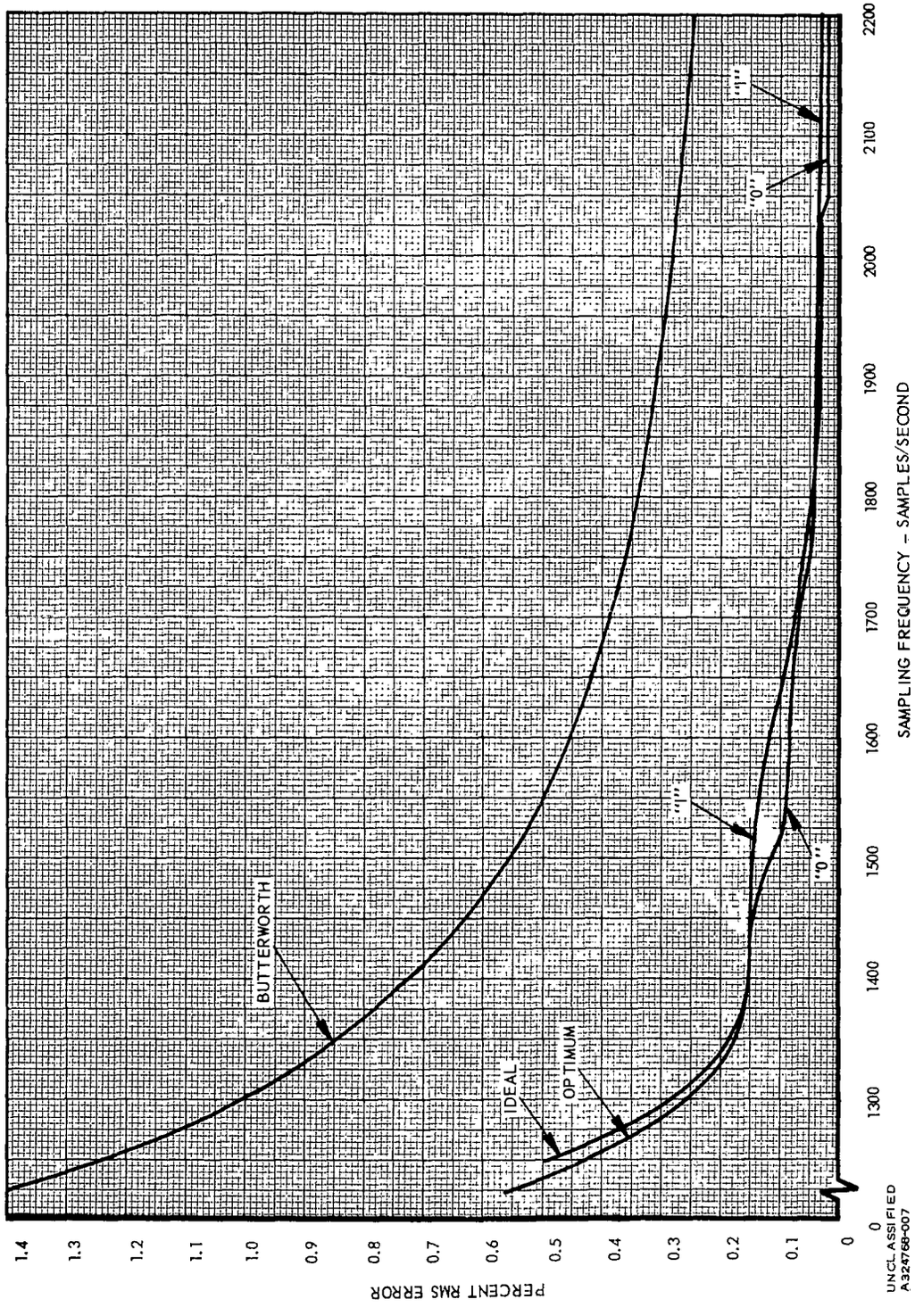

Figure 3-4 Aliasing Error vs Sampling Frequency - High Resolution Channels: Expanded (Cosine-Squared Input Function)

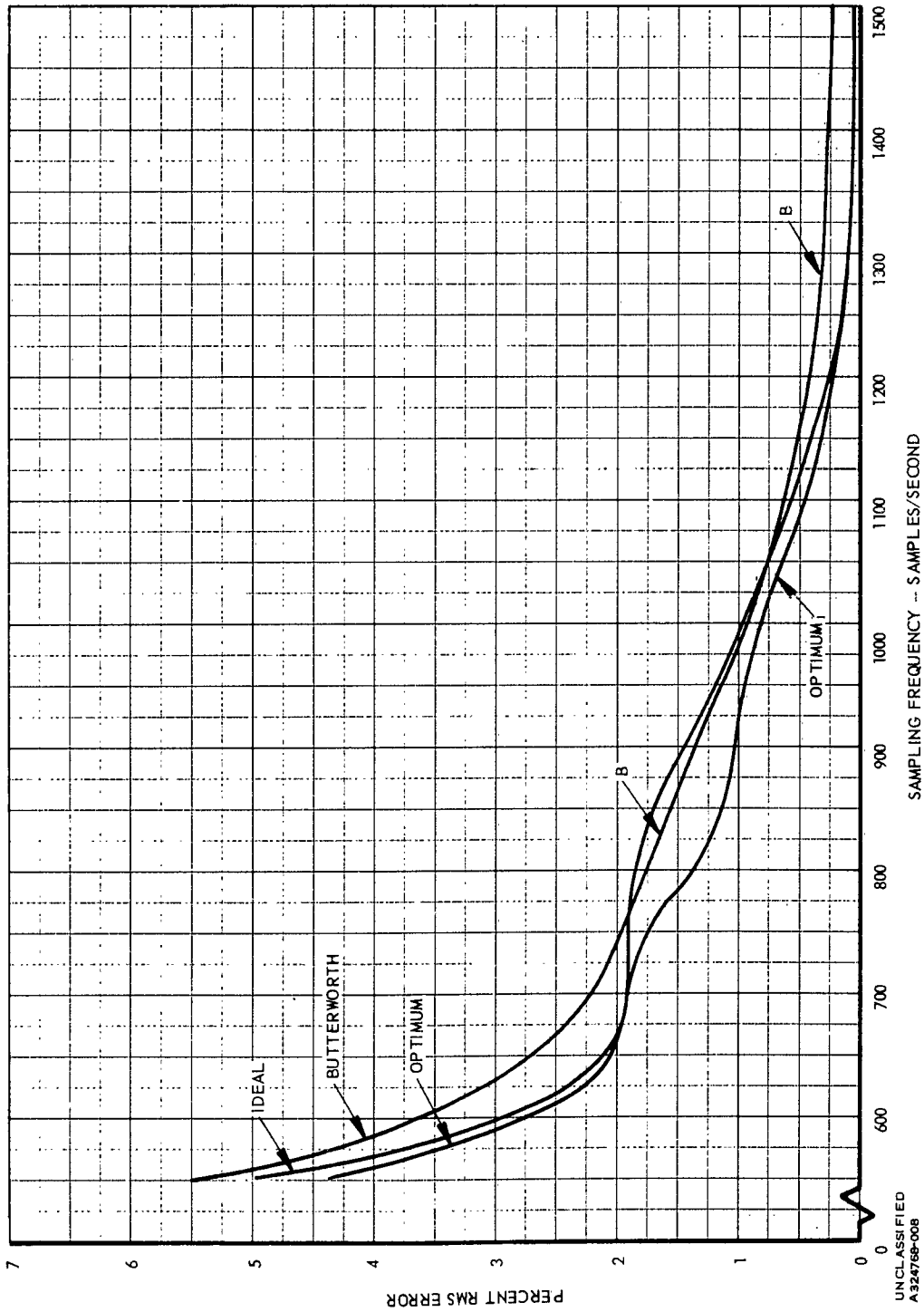

Figure 3-5 Aliasing Error vs Sampling Frequency - Low Resolution Channels (Gaussian Input Function)

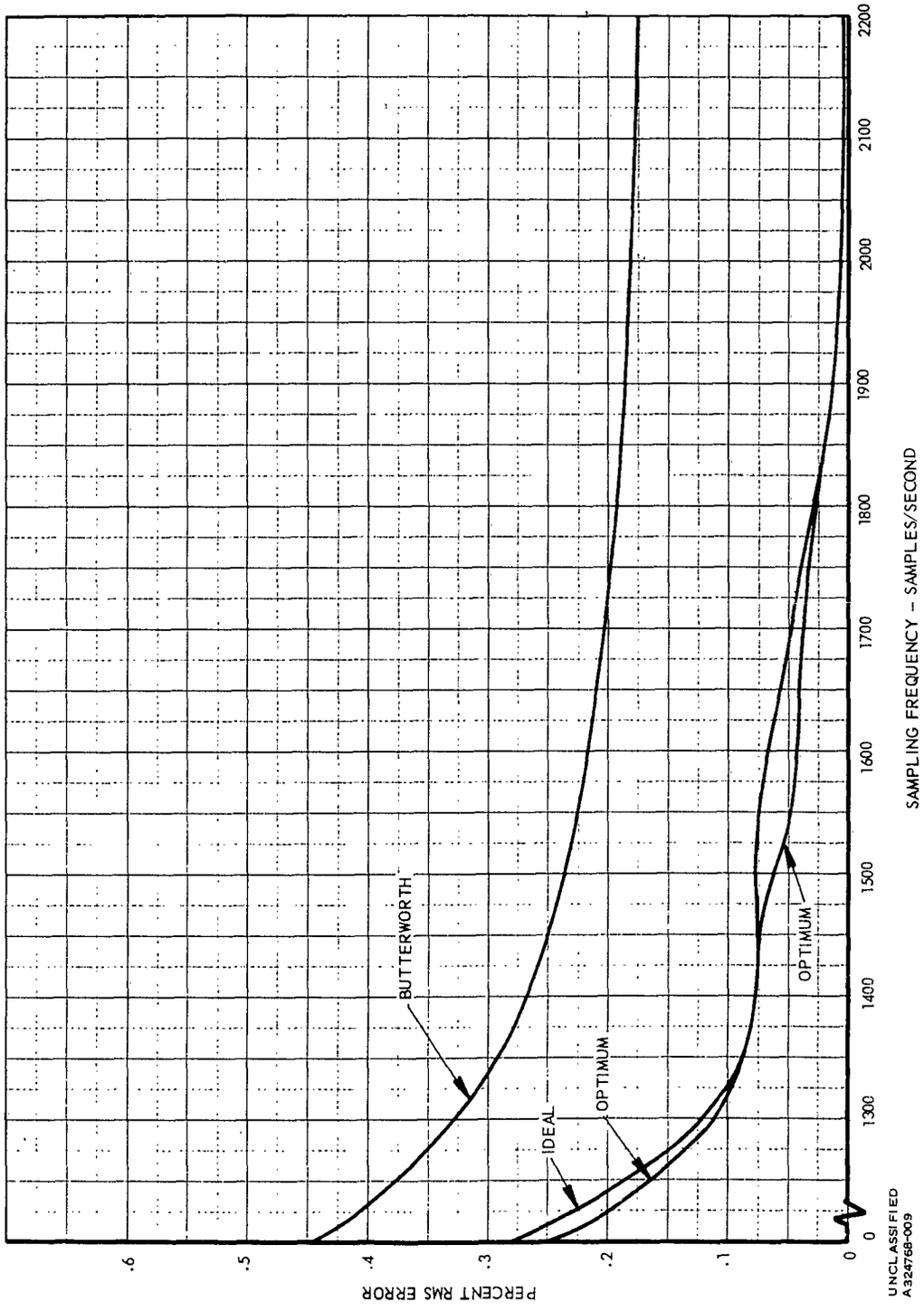

Figure 3-6 Aliasing Error vs Sampling Frequency - Low Resolution Channels: Expanded (Gaussian Input Function)

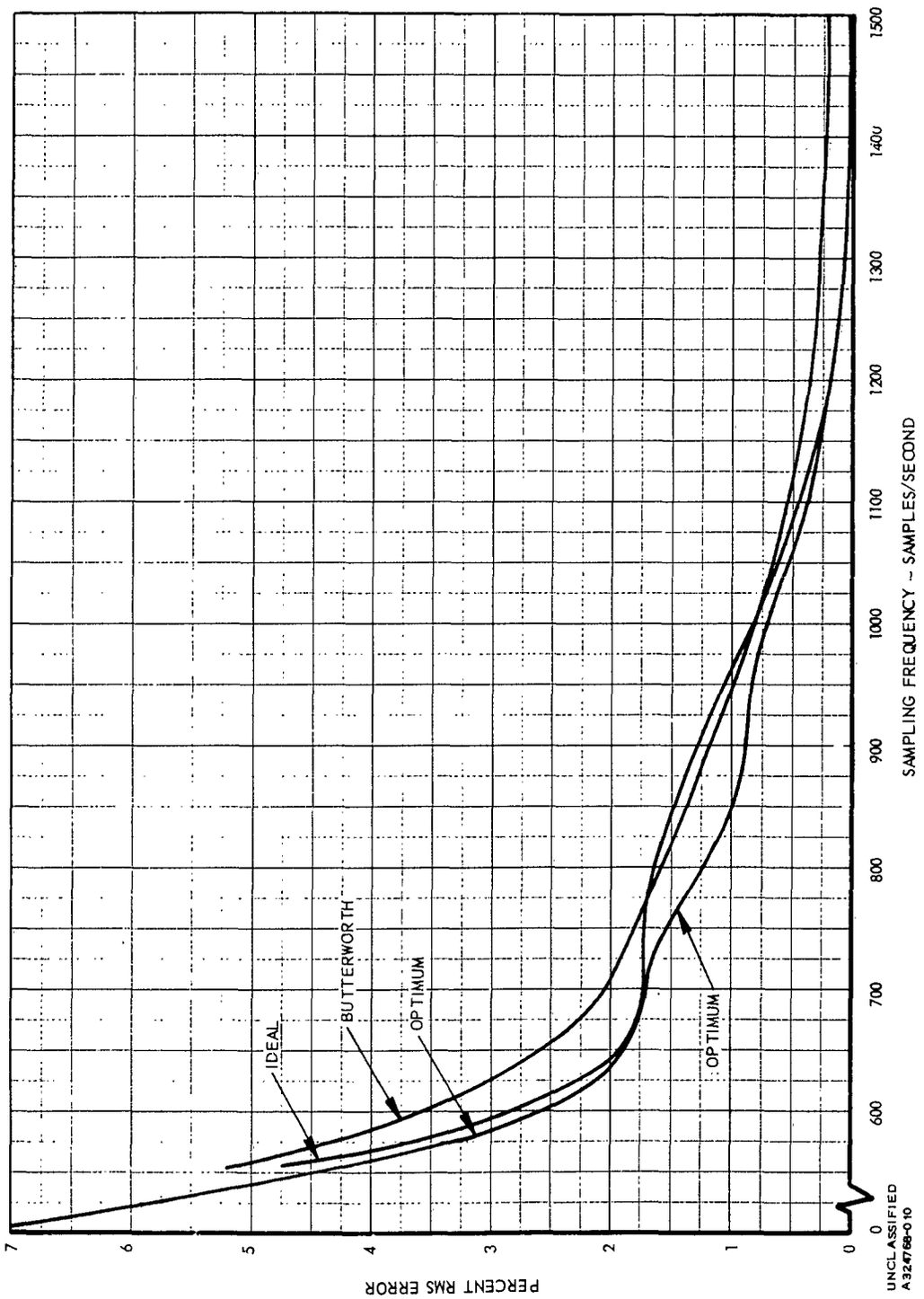

Figure 3-7 Aliasing Error vs Sampling Frequency - Low Resolution Channels (Cosine-Squared Input Function)

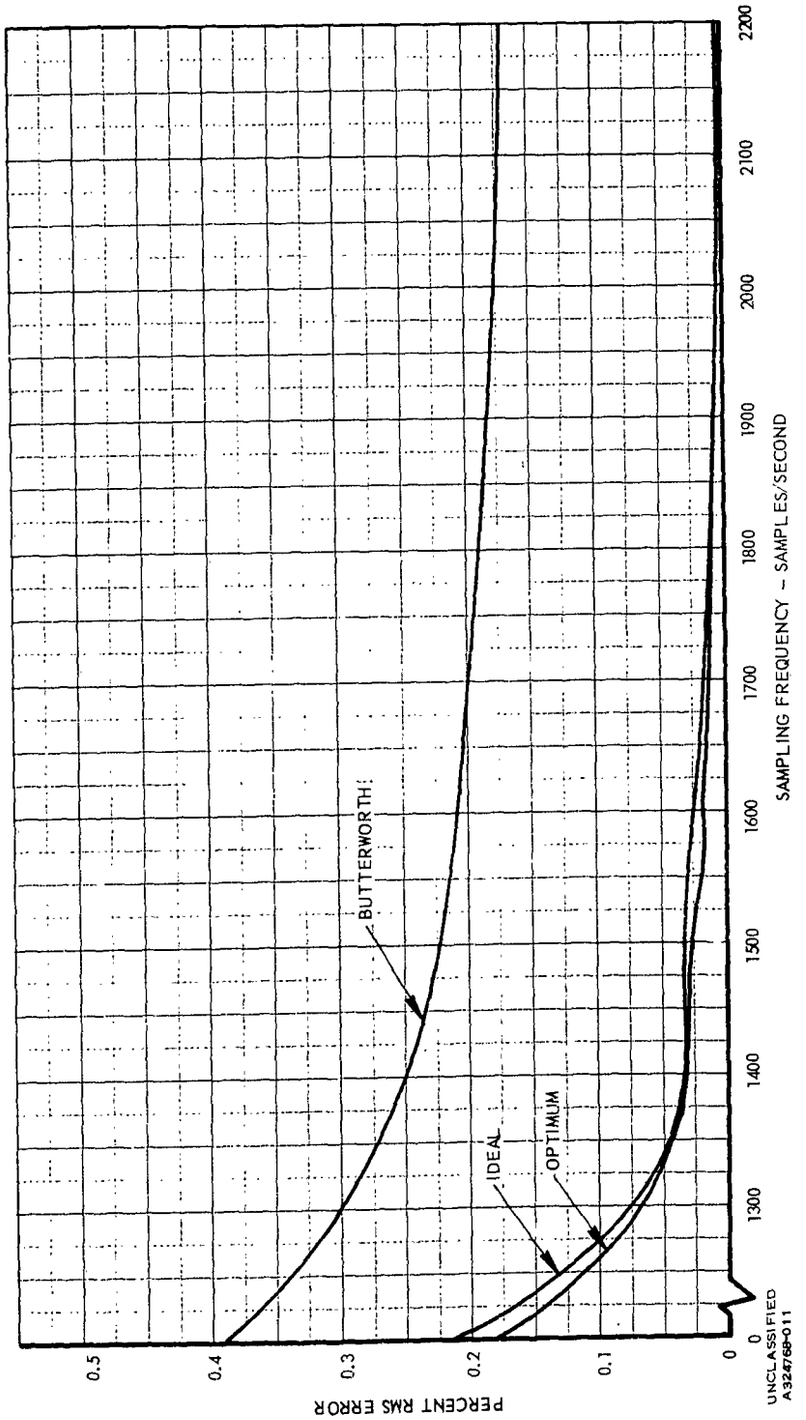

Figure 3-8 Aliasing Error vs Sampling Frequency - Low Resolution Channels: Expanded (Cosine-Squared Input Function)

3.2 EFFECT OF CHANGING AMPLIFIER ROLL-OFF

If the amplifier-detector high frequency roll-off is increased to 24 db/octave, a significant reduction of error is achieved. Figure 3-9 shows the results of the computer analysis for this assumption with a Gaussian input function to the high resolution channels, and an ideal interpolation filter. For the same sampling frequency, the aliasing error is reduced approximately 50 percent. This should have been immediately obvious since the area under this portion of the curve is reduced by one-half when the slope is doubled.

3.3 EFFECT OF CHANGING THE INTERPOLATION FILTER CUT-OFF

For a constant sampling frequency, the cut-off frequency of the ideal and Butterworth filters was varied about half the sampling frequency. The computer results indicated that minimum error occurred for a cut-off at $f_s/2$.

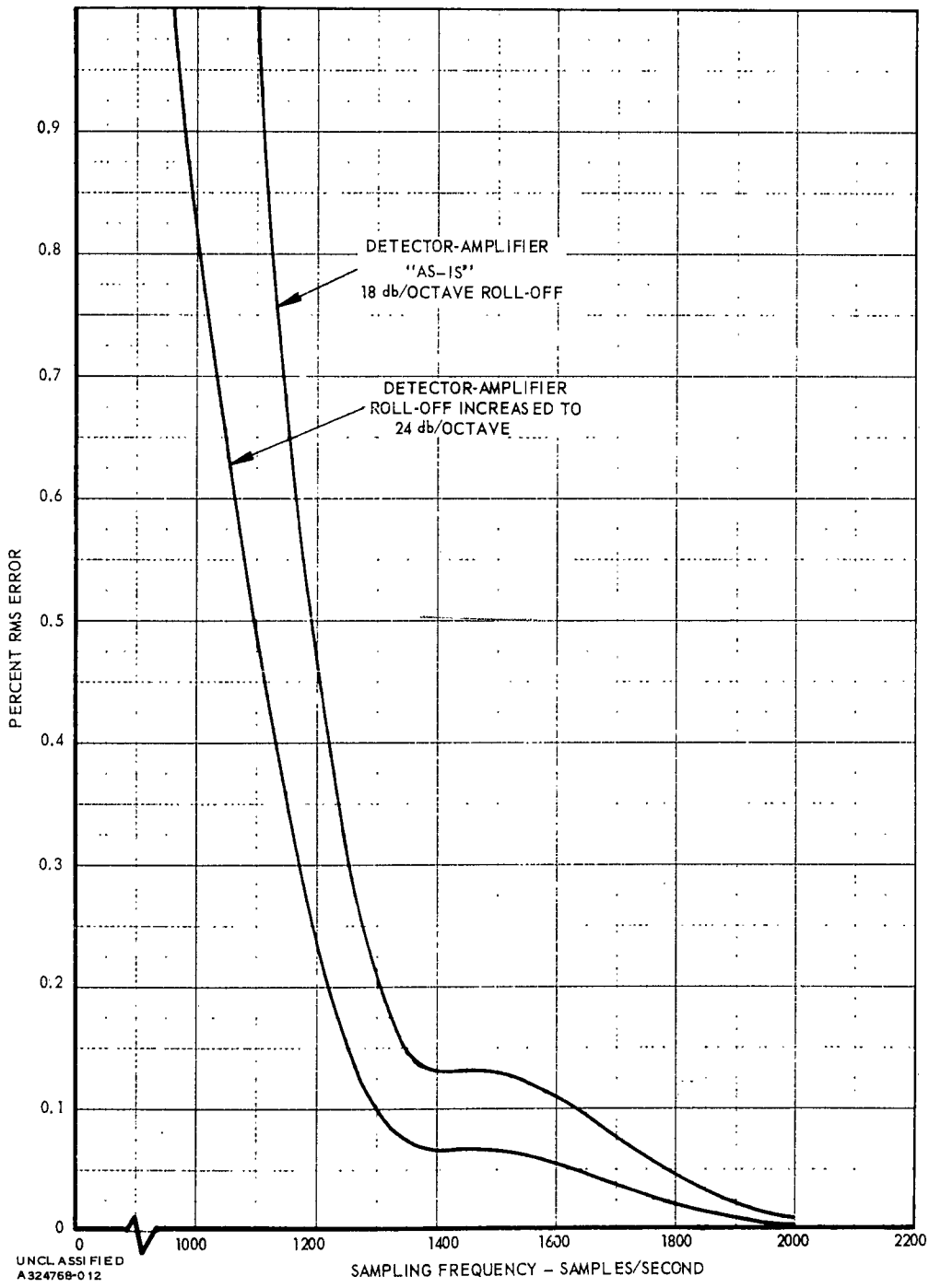

Figure 3-9 Effect of Increasing Amplifier-Detector Roll-Off (Aliasing Error vs Sampling Frequency - High Resolution Channels: Gaussian Input Function)

SECTION 4
NUMBER OF HIGH VS NUMBER OF LOW RESOLUTION CHANNELS

The data spectra used in this study are typical of the high and low resolution sensors, and since high accuracy is desired, the aliasing error must be minimized. Since the Gaussian input function is a "worst-case" condition, it will be used in calculating the number of channels.

For a seven-bit PCM system, the maximum commutation rate is 114 Kc as dictated by the 800 kilo-bit maximum rate set by IRIG. Therefore, the number of channels that can be multiplexed is:

$$N = \frac{114,000}{f_s}$$

where f_s is the sampling rate per channel.

Since f_s is dictated by the tolerable aliasing error, the number of channels could easily be determined were it not for the difference in sampling rates required by the high and low resolution channels for the same aliasing error.

For example: if 0.3 percent rms aliasing error is tolerable it is indicated (Figure 3-2) that 1700 sps should be used for the high resolution channels, and that 1190 sps (Figure 3-5) should be used for the low resolution channels. Therefore, in order to operate in an efficient manner, the high and low resolution channels should be sampled at a rate of $\frac{1700}{1190}$ or $\frac{10}{7}$. Because this would require an overly complex multiplexer design, the 1:1 sampling ratio (although inefficient) is desirable. With this arrangement, the number of channels is dictated by the tolerable aliasing error of the high resolution channels For a 0.3 percent error the total number of channels is 67.

Super-commutation may be employed providing the allowable aliasing error for the low resolution channels is relaxed to that value corresponding to half the sampling rate of the high resolution channels. If 0.3 percent aliasing error is tolerable, the sampling rate (Figure 3-2) is 1700; therefore, at a sampling rate of 850 for the low resolution channels the aliasing error for the channels (Figure 3-5) is 1.7 percent.

If super-commutation, twice-per-frame, is utilized for the high resolution channels, the total number of channels is given by

$$N = 2H + L$$

Where H is the number of high resolution channels, N is the number of low resolution channels, and the total number of channels is determined by the sampling rate of the low frequency channels. In the case cited:

$$N = \frac{114,000}{850} = 134$$

Figure 4-1 indicates the number of high vs the number of low resolution channels for the foregoing assumption.

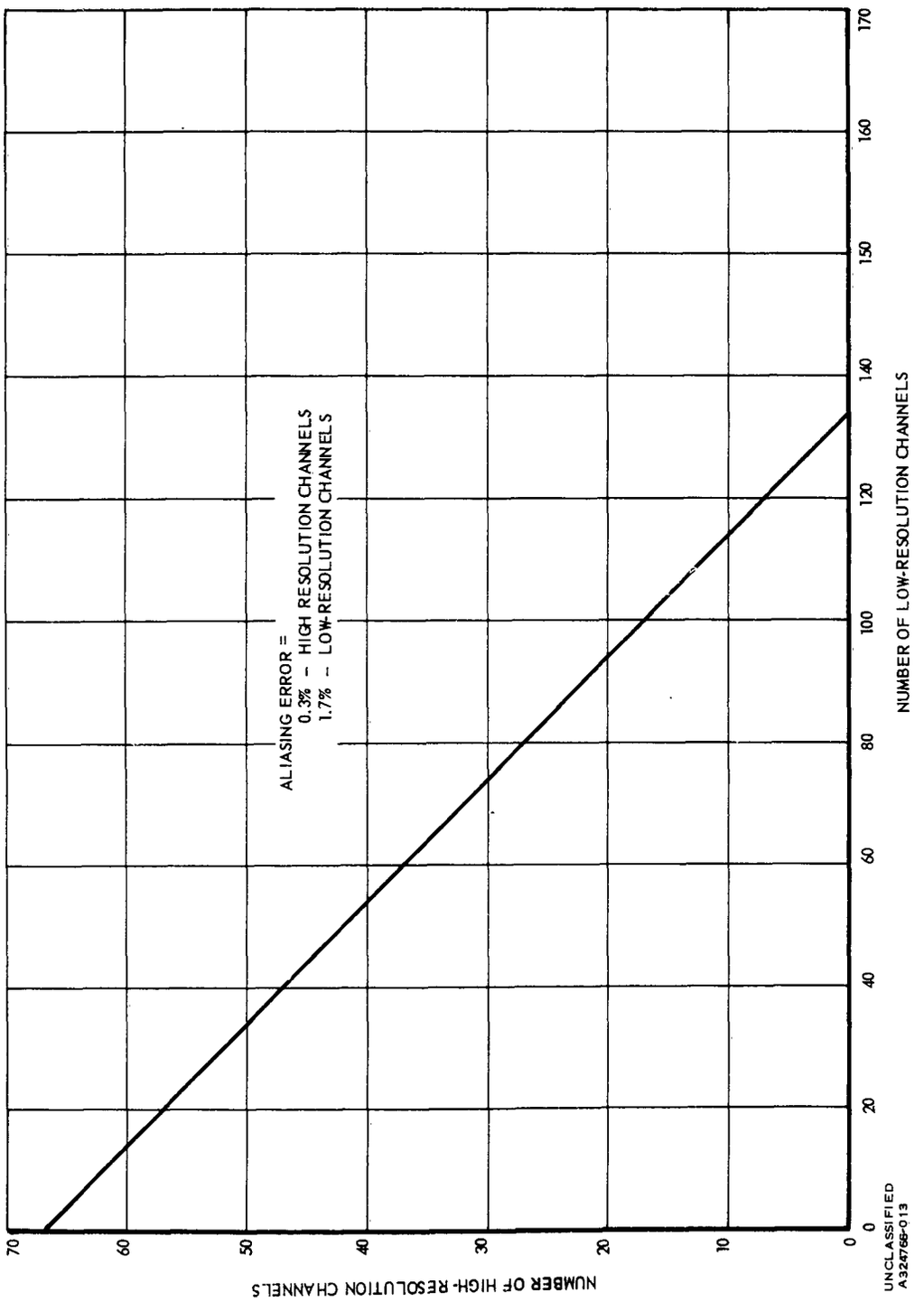

Figure 4-1 Number of High vs Number of Low Resolution Channels (Gaussian Input Function, Ideal Interpolation Filter, and Super Commutation of High Resolution Channels)

SECTION 5
CONCLUSIONS AND RECOMMENDATIONS

5.1 CONCLUSIONS

Results of the analysis indicate that the assumption of a Gaussian function for the blur-circle gives a "worst-case" condition. Therefore, pertinent conclusions should be drawn from Figures 3-2, 3-5, and 3-6 using the curve for the ideal interpolation filter. It is also indicated that super-commutation, twice-per-frame, can be employed if the accuracy requirements are relaxed for the low resolution channels thereby allowing a greater total number of channels. If once-per-frame commutation is used, the total number of channels is 67 for a 0.3 percent maximum aliasing error at 114 Kc commutation rate. This condition is wasteful of bandwidth if utilized to telemeter the low resolution channels. When twice-per-frame super-commutation is employed, the total number of channels is increased to 134, but the aliasing error of the low resolution channels is increased to 1.7 percent.

By modifying the transfer function of the detector-amplifier to increase the roll-off to 24 db/octave, the aliasing error is reduced approximately 50 percent.

5.2 RECOMMENDATIONS

Since the study is based on the assumption that the actual blur circle function is somewhere between Gaussian and cosine-squared, it is recommended that a laboratory experiment be devised to determine the actual function. The amplifier-detector transfer function could also be made more precise if the unit were constructed and frequency response measurements performed. With these improvements in the transfer functions the aliasing error analysis should be re-run with other refinements such as inclusion of detector and thermal noise.

Under consideration at the present time is the effect of detector noise on the results of the analysis. Work should continue in order to determine the mathematical function which best describes the noise spectral density and how to treat the combination of signal and noise statistically as it is passed through the system.

Consideration should also be given to increasing the roll-off of the amplifiers from 18 db/octave to 24 or 30 db/octave. It is recognized that the penalty for doing this is increased complexity with all its ramifications, but the outcome is great, as witnessed by the curves in Figure 3-5.

Since the total number of telemetry channels is sharply reduced if the accuracy requirements are identical for the high and low resolution channels, the feasibility of relaxing the low resolution accuracy requirement should be investigated.

APPENDIX A

DERIVATION OF THE PARAMETERS FOR COSINE-SQUARED PULSE

Given:

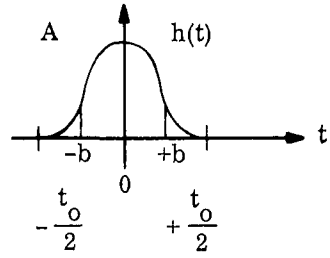

$$h(t) = A \cos^2 \pi \frac{t_o}{t}, \quad -\frac{t_o}{2} \leq t \leq +\frac{t_o}{2}$$

$$= 0, \text{ elsewhere}$$

95 percent of energy (area) lies between -b and +b, and the time between -b and +b $= \frac{1}{720}$ second

Find: t_o in terms of b

Solution:

$$\text{Total Area} = A \int_{-\frac{t_o}{2}}^{+\frac{t_o}{2}} \cos^2 \pi \frac{t}{t_o} \, dt = \frac{A}{2} \left[t + \frac{t_o}{2\pi} \sin \frac{2\pi}{t_o} t \right]_{-\frac{t_o}{2}}^{+\frac{t_o}{2}}$$

$$= A \frac{t_o}{2}$$

$$\text{Area between } -b \text{ and } +b = \frac{A}{2}\left[t + \frac{t_o}{2\pi}\sin\frac{2\pi}{t_o}t\right]_{-b}^{+b}$$

$$0.95\,A\frac{t_o}{2} = A\left[t + \frac{t_o}{2\pi}\sin\frac{2\pi}{t_o}t\right]^{b}$$

$$0.95\,A\frac{t_o}{2} = A\left[b + \frac{t_o}{2\pi}\sin\frac{2\pi}{t_o}b\right]$$

This is a transcendental function; for which the approximate solution is:

$$b = 0.34\,t_o$$

Since the time between -b and +b is $\frac{1}{720}$ second;

$$t_o = \frac{1}{490} \text{ second}$$

APPENDIX B
EFFECT OF FINITE DWELL TIME

It is shown (Ref 1) that the error caused by frequency distortion, introduced by finite sampling, is given by:

$$E\left(f\right) = 1 - \frac{\sin \pi f \tau}{\pi f \tau}$$

Where:

f is the highest frequency of interest in the data, which in this case is assumed to be the Nyquist frequency $f_{s/2}$, typically 850 cps; and τ is a sample duration. For a 114 Kc commutation rate, 100 percent duty cycle multiplexer:

$$\tau = \frac{1}{114,000}$$

Therefore, the error at 1840 cps is:

$$1 - 0.99996 \text{ or } 0.004 \text{ percent}$$

REFERENCES

1. FACT Report No. 6, PAM System Capability (U), LMSC-A315884, 14 February 1963 (Confidential).

2. Spilker, J. J., Optimization and Evaluation of Sampled Data Filters, LMSD-48335, 18 November 1958.

3. Stiltz, Aerospace Telemetry, Appendix 4A, Prentice Hall.

DISTRIBUTION

Addressee	Quantity
AFSSD (SSZM) Attn: Col. L. S. Norman Air Force Unit Post Office Los Angeles 45, California	5
Aerospace Corporation Attn: J. Statsinger 2400 East El Segundo Blvd. El Segundo, California	3
Defense Documentation Center Arlington Hall Station Arlington 12, Virginia	10
Air Force Plant Representative Attn: Dave Meeker P. O. Box 504 Sunnyvale, California	1
LMSC Organizations	33
	52

DR